Constraints on Ω_b from nucleosynthesis of ^{7}Li in the standard big bang model

A. Coc, E. Vangioni-Flam, M. Casse, M. Rabiet

Constraints on Ω_b from nucleosynthesis of ^{7}Li in the standard big bang model

Alain Coc
Centre de Spectrométrie Nucléaire et de Spectrométrie de Masse, IN2P3-CNRS and Université Paris Sud, Bâtiment 104, 91405 Orsay Campus, France

Elisabeth Vangioni-Flam
Institut d'Astrophysique de Paris, 98 bis Bd Arago, 75014 Paris, France

Michel Cassé
Service d'Astrophysique, DAPNIA, DSM, CEA, Orme des Merisiers, 91191 Gif sur Yvette CEDEX, France and Institut d'Astrophysique de Paris, 98 bis Bd Arago, 75014 Paris, France

Marc Rabiet
Institut d'Astrophysique de Paris, 98 bis Bd Arago, 75014 Paris, France
(Received 1 October 2001; published 24 January 2002)

We update standard big bang nucleosynthesis (SBBN) calculations on the basis of recent nuclear physics compilations (NACRE in particular), experimental and theoretical works. By a Monte Carlo technique, we calculate the uncertainties on the light element yields (^{4}He, D, ^{3}He and ^{7}Li) related to nuclear reactions. The results are compared to observations that are thought to be representative of the corresponding primordial abundances. It is found that ^{7}Li could lead to more stringent constraints on the baryonic density of the universe ($\Omega_b h^2$) than deuterium, because of much higher observation statistics and an easier extrapolation to primordial values. The confrontation of SBBN results with ^{7}Li observations is of special interest since other independent approaches have also recently provided $\Omega_b h^2$ values: (i) the anisotropies of the cosmic microwave background by the BOOMERANG, CBI, DASI and MAXIMA experiments and (ii) the Lyman-α forest at high redshift. A comparison between these results obtained by different methods provides a test of their consistency and could provide a better determination of the baryonic density in the universe. However, the agreement between $\Omega_b h^2$ values deduced from SBBN calculation and ^{7}Li observation on the one hand and CMB observations on the other hand is only marginal.

DOI: 10.1103/PhysRevD.65.043510 PACS number(s): 26.35.+c, 98.80.Ft

I. INTRODUCTION

Recently, different ways to determine the baryonic density of the universe have been exploited. Here, we use the usual notation where Ω_b denotes the ratio of the baryon density over the critical density of the universe, and η is the baryon over photon ratio. They are related by $\Omega_b h^2 = 3.65 \times 10^7 \eta$ with h the Hubble constant in units of 100 km s^{-1} Mpc^{-1}. It is now possible to confront the results of these different approaches to test the validity of the underlying model hypothesis and hopefully obtain a better evaluation of this crucial cosmological parameter. Three independent methods have been used so far to derive the baryon density of the universe: (i) the pioneering one, (standard) big-bang nucleosynthesis (SBBN), based on nuclear physics in the early universe, (ii) very recently, the study of the cosmic microwave radiation (CMB) anisotropies and (iii) the census of H (and also He$^+$) atomic lines from the Lyman-α forest at high redshift.

Regarding the uncertainties attached to each of these methods, those related to SBBN are probably the best controlled. Standard BBN depends essentially on one parameter, η, the baryon to photon ratio since the number of light neutrinos is essentially known. This model, in its standard version, has survived for many decades showing its robustness. It success in reproducing the light element (^{4}He, D, ^{3}He, and ^{7}Li) primordial abundances over a span of 10 orders of magnitude is remarkable [1]. The leading uncertainties come from the observations of the isotopes in different astrophysical sites and the way they are interpreted (D in particular) to estimate the primordial abundances and the insufficient knowledge of some reaction rates. Lithium suffers from two drawbacks: (i) it is affected more than any other light isotope by uncertainties in the nuclear reaction rates and (ii) the valley shape in its abundance versus η curve leads to two possible η values for a given abundance. This shape is due to its production modes, by ^{3}H+^{4}He and ^{3}He+^{4}He, respectively at low and high baryonic density. The first difficulty could be reduced by a better determination of a few key cross sections, but the second one is intrinsic to the calculation. Thus to remove the degeneracy on the baryon density, lithium should be associated with, at least, one other light element, deuterium for instance. However, the relation between ^{7}Li observations and its primordial abundance seems more straightforward than for D.

In the case of the CMB, the $\Omega_b h^2$ values deduced from observations tend to converge but their interpretations are probably still model dependent. The CMB analyses involve many parameters, principally the various energy densities (Ω_{tot}, Ω_b, Ω_Λ, respectively the total density, baryonic density and the cosmological constant contribution), h, the initial fluctuation spectrum index (n_s), the reionization optical depth (τ_c) and the overall normalization. The baryon density is extracted from the amplitudes of the acoustic peaks in the angular power spectrum of the CMB anisotro-

pies. It is important to note that the ratio of amplitudes between the first and second peaks increases with Ω_b, in contrast with all other cosmological parameters. Hence, the determination of $\Omega_b h^2$ does not suffer from the cosmic degeneracy that affects Ω_Λ and Ω_m and a high precision can be expected [2]. However, these values are obtained in the framework of inflationary models that could be altered in other cosmological contexts [3].

The third method is based on the study of the atomic H I and He II Lyman-α absorption lines observed in the line of sight of quasars. Quasars being the brightest objects of the universe, they can be observed at very large redshift. On their line of sight, atoms both in diffuse or condensed structures absorb part of their radiation, making absorption lines apparent. It allows in particular to study the intergalactic medium via the so-called Lyman-α forest. This method leads to an estimate of the baryon content of the Universe on large scales [4,5]. Indeed, the evaluation of $\Omega_b h^2$ through the study of the evolution of the Lyman-α forest in the redshift range $0<z<5$, though indirect because of the relatively large ionization uncertainties, leads to results consistent with the two previous methods.

In the following, we update the big bang nucleosynthesis calculations on the basis of the recent NACRE compilation [6] of reaction rates supplemented by other recent works [7–9]. We performed Monte Carlo calculations to estimate the uncertainties on light element yields arising from nuclear reactions alone. Similar calculations have been performed recently, based on a different compilation and analysis of nuclear data (Nollett and Burles [10], and Cyburt *et al.* [11]). However, here, we put the emphasis on ^{7}Li as its primordial abundance is more reliable than that of other light isotopes (D in particular). Using ^{7}Li as the main *baryometer* one deduces $\Omega_b h^2$ and we compare it with (i) with the helium and deuterium primordial abundances, (ii) other SBBN investigations and (iii) independent evaluations (CMB and Lyman-α forest).

II. OBSERVATIONAL CONSTRAINTS FROM THE LIGHT ELEMENTS

Here we present the selection of astrophysical observations that we use for the determination of the baryon density of the Universe from the SBBN calculation. To estimate primordial abundances, observations are made on the oldest objects that are characterized by their high redshift z or low *metallicity*.[1]

The determination of the primordial ^{4}He abundances is derived from observations of metal-poor, extragalactic, ionized hydrogen (H II) regions. This extraction is difficult to the level of precision required, due to the incomplete knowledge of the different atomic parameters involved. Olive and Skillman [12] have studied in great detail the systematic uncertainties, and concluded that the typical errors given in previous studies are underestimated by a factor of about two. The extreme values published [13–15] cover the range fom 0.231 to 0.246 (in mass fraction), putting little constraint on models. Consequently, in this work, ^{4}He will not be considered as a discriminating indicator of the baryonic density.

Deuterium is peculiar because, after BBN, this fragile isotope, can, in principle, only be destroyed in subsequent stellar or galactic nuclear processing. Hence the primordial abundance should be represented by the *highest* observed value. It is measured essentially in three astrophysical sites: (i) in the local interstellar medium (present value), (ii) in the protosolar cloud (4.6 Gyr ago) and (iii) in remote cosmological clouds on the line of sight of high redshift quasars (large lookback time). In principle, the later sample (iii) should be the closest representative of the primordial D value, but up to now, the observations lead to two ranges of D abundance values. However, very recently, it has been shown [16] that the D abundance on the line of sight of the quasistellar object (QSO) PG1718+4607 cannot be determined due to blending between the Lyman-α and the main hydrogen absorption lines, contrary to a previous study [17]. Since this observation was the main evidence for a high D/H value ($\sim 10^{-4}$ corresponding to a low η range; see for instance Ref. [18]), the very high primordial D abundance seems to have lost its support and hence only one range of (low) D/H values remains. However, the D abundance data from cosmological clouds remain scarce and scattered (Fig. 1, upper panel). The extreme values deduced from the different observations [20–23] lead to the interval $1.3\times10^{-5}<\mathrm{D/H}<4.65\times10^{-5}$ (including error bars). This dispersion (amounting to a factor of about 3), if physical and not observational, casts a doubt on the direct identification of the observed values with the primordial D abundance. Alternatively, it could indicate that this fragile isotope has already been processed in these high redshift clouds despite their low metallicity [19]. Thus, in this perspective, averaging the D/H abundances measured in cosmological clouds to infer the primordial value seems somewhat inappropriate. In addition the observations of the absorbing cloud on the line of sight of QSO 0347-3818 have been analyzed using two methods [22,24] and lead to different values (stars in Fig. 1). This suggest that systematic errors may still be important.

On the other hand, it has been shown [25] that there exists a large dispersion in the local measurements [$(0.5$ to $4)\times10^{-5}$]. This could indicate that unknown processes are at work to modify the D abundance at small scale in our Galaxy. Thus, if it is confirmed that local D abundances are scattered as the result of yet unknown physical processes, the same thing could occur in absorbing clouds at large redshift. In addition, the lowest value obtained at high redshift [23] [$\mathrm{D/H}=(1.65\pm0.35)\times10^{-5}$] is uncomfortably close to both the solar system and interstellar ones (respectively around 2.1×10^{-5} and 1.5×10^{-5} [26,27,25]). It is inconsistent with

[1]Metallicity represents the abundance of *metals* which, in the astrophysical language, corresponds to all elements above helium. As metallicity increases in the course of galactic evolution, this is an indicator of the age of an object. Abundances of common elements like Fe (or e.g. Si), are often taken as representative of the metallicity. The notation $[\mathrm{Fe/H}]\equiv\log(\mathrm{Fe/H})_{\mathrm{star}}-\log(\mathrm{Fe/H})_\odot$ is often used. For instance, $[\mathrm{Fe/H}]=-2$ corresponds to 1% of the solar ($\odot$) metallicity. Otherwise, D/H or ^{7}Li/H for instance, represent the ratio of abundances by number of atoms.

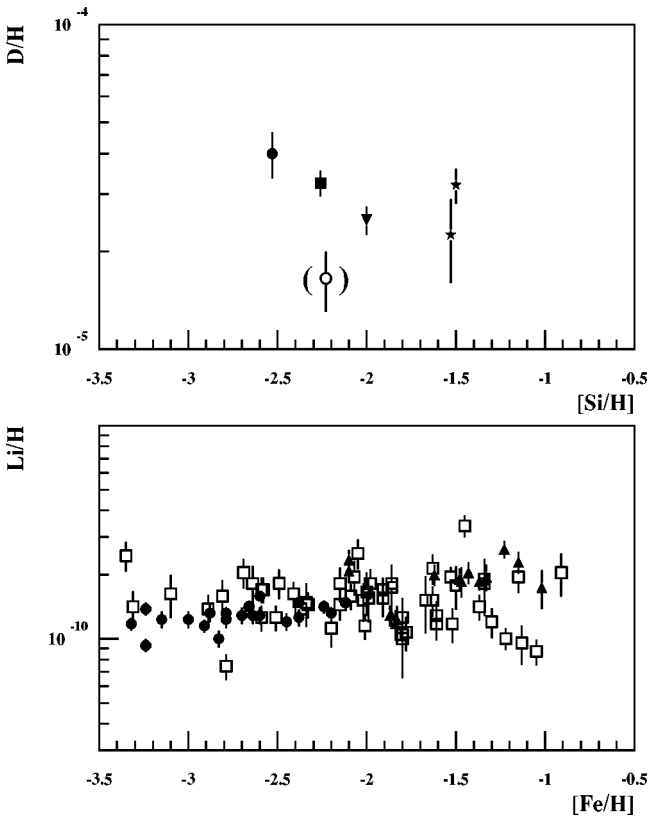

FIG. 1. Observed abundances as a function of metallicity from objects which are expected to reflect primordial abundances. Upper panel: observed D abundances, from Refs. [20,21,23,22,24] (stars corresponding to two analyses of observations of the same cloud [22,24]). Lower panel: observed ^{7}Li abundances, circles [32] and triangles [31] from Ryan *et al.*; squares from Bonifacio and Molaro [30].

even the most conservative galactic evolution models since it would require a negligible D destruction. Note that this lowest value [23] (in parenthesis in Fig. 1) is affected by a large uncertainty concerning the level of the continuum and the blending of the relevant lines [28]. If this questionable observation is put aside, a trend appears in the D/H data versus metallicity [Si/H] (Fig. 1) showing a D abundance decreasing when metallicity increases, as qualitatively expected from stellar evolution [19]. (To view the trend we do not consider the alternative analysis [24] of QSO 0347-3818 to be consistent with the analyses of the other observations.) Accordingly, the true primordial D/H value should be obtained from extrapolation to zero metallicity. Consequently, even though, in principle D better constrains η than ^{7}Li (U shape of the curve), the value of its primordial abundance is still a matter of debate. We adopted the highest observed value [20] in a cosmological cloud assuming that lower values are the result of subsequent processing.

Compared to D, the determination of the ^{7}Li primordial abundance from observations leaves less room for interpretations. Since the discovery of a plateau in the lithium abundance as a function of metallicity (Fig. 1, lower panel), drawn for metal poor dwarf stars [29], many new observations have strengthened its existence. The fact that the abundance does not increase with time (metallicity) at the surface of the oldest stars was interpreted as being representative of the primordial ^{7}Li abundance [30–32]. As such, these measurements could have been affected by two processes (i) a production related to nonthermal (spallation) nuclear reactions (mainly $\alpha+\alpha$) in the interstellar medium, increasing the amount of lithium in forming stars at a given metallicity and (ii) a depletion in the envelope of these stars. The contribution of the first process is small at very low metallicity amounting typically to less than 10% at a metallicity $[\mathrm{Fe/H}]=-2$ [33]. At $[\mathrm{Fe/H}]=-1$, this contribution is more significant but remains within the dispersion of the data. The second one concerns the potential depletion of lithium by nuclear destruction and possibly by diffusion and rotational mixing [34]. The small scatter of the data, over three metallicity decades, on the one hand and the presence of the even more fragile ^{6}Li isotope in a few halo stars (e.g., Ref. [35]) on the other hand, strongly limit the amount of possible depletion. Hence, this effect should also be within the dispersion of the data. Bonifacio and Molaro [30] have deduced from their large observational sample a primordial value: $\log(\mathrm{Li/H})=-9.762\pm0.012$ (statistic, 1σ) ±0.05 (systematic). More recently, Ryan *et al.* [31,36], on the basis of their observations, have provided a new determination: $^7\mathrm{Li/H}=(1.23^{+0.68}_{-0.32})\times10^{-10}$. Their mean value and (95% confidence) limits take into account all possible contributions from ^{7}Li depletion mechanisms and bias in analysis. But the main difference with the earlier work [30] is that they have taken into account a slight rise of the lithium abundance due to spallation reaction leading to a smaller primordial abundance when extrapolated a zero metallicity. Accordingly, we adopt their range for the primordial ^{7}Li abundance.

III. CMB AND LYMAN-α FOREST OBSERVATIONS

CMB anisotropy measurements give independent estimates of the baryonic density of the Universe. The first determinations of $\Omega_b h^2$ from BOOMERANG and MAXIMA [37–39] yielded $\Omega_b h^2\approx0.03$. The Cosmic Background Imager (CBI), ground based, has given preliminary results in marked contrast [40] ($\Omega_b h^2\approx0.009$) to BOOMERANG-MAXIMA values. The Degree Angular Scale Interferometer, DASI (along with its sister instrument CBI) [41], is one of the new compact interferometers specifically built to observe the CMB. Combined with the large angle measurements made by the Cosmic Background Explorer (COBE), it has been able to reveal a significant signal in the second peak region and has determined $\Omega_b h^2=0.022^{+0.004}_{-0.003}$ (1σ). Recently, new analyses [42,43] of BOOMERANG data have also led to $\Omega_b h^2=0.022^{+0.004}_{-0.003}$ (1σ). But the situation is not yet settled and a wealth of new data is expected from future ground instruments, long balloon flights and especially satellites [Microwave Anisotropy Probe (MAP), Planck Surveyor].

As mentioned above, the study of the baryon content of the intergalactic medium evolution of the Lyman-α forest in the redshift range $0<z<5$ leads to an evaluation of $\Omega_b h^2$. Such analyses have lead to $\Omega_b h^2\geqslant0.0125$ [4,28] and $\leqslant0.03$ [4,5,28]. Hui *et al.* [44] using recent observations [45,46]

TABLE I. Influential reactions and their sensitivity to nuclear uncertainties for the production of ^{4}He, D, ^{3}He, and ^{7}Li in SBBN. [$\Delta N/N \equiv N_h/N_l - 1$; n.s.: not significant ($|\Delta N/N| < 0.01$).]

Reaction \ $\Delta N/N$	^{4}He	D	^{3}He	^{7}Li
^{1}H$(n,\gamma)^2$H[a]	n.s.	n.s.	n.s.	0.08
^{2}H$(p,\gamma)^3$He	n.s.	-0.19	0.19	0.26
^{2}H$(d,n)^3$He	n.s.	-0.09	0.06	0.12
^{2}H$(d,p)^3$H	n.s.	-0.03	-0.04	0.01
^{3}H$(d,n)^4$He	n.s.	n.s.	n.s.	-0.07
^{3}H$(\alpha,\gamma)^7$Li	n.s.	n.s.	n.s.	0.24
^{3}He$(n,p)^3$H[b,d]	n.s.	n.s.	-0.06	-0.03
^{3}He$(d,p)^4$He[c,d]	n.s.	n.s.	-0.12	-0.12
^{3}He$(\alpha,\gamma)^7$Be	n.s.	n.s.	n.s.	0.39
^{7}Li$(p,\alpha)^4$He	n.s.	n.s.	n.s.	-0.25
^{7}Be$(n,p)^7$Li[c,d]	n.s.	n.s.	n.s.	-0.13

[a]Chen and Savage [9].
[b]Brune *et al.* [8].
[c]Smith, Kawano, and Malaney[7].
[d]$\pm 1\sigma$ variation.

have found $\Omega_b h^2 h = 0.03 \pm 0.01$. These various results are summarized in Table II, compared in Fig. 5 and discussed in Sec. V.

IV. NUCLEAR DATA

Most of the important reactions for ^{7}Li production (Table I) are available in the NACRE compilation of thermonuclear reaction rates [6]. Other reactions in our BBN network are adapted from an earlier compilation [7] or more recent works [8,9]. In our previous studies, we have studied the influence of individual reactions [18] or extreme yield limits [48] obtained when considering all combinations of low and high rates. Here, instead, we have performed Monte Carlo calculations to obtain statistically better defined limits, as we did in a previous work [49] that was limited to the NACRE reactions. Here we update these calculations by taking into account uncertainties on the remaining reactions. In the following, we discuss the origin of these calculated uncertainty limits.

One of the main innovative features of NACRE with respect to former compilations [50] is that uncertainties are analyzed in detail and realistic lower and upper bounds for the rates are provided. Using these low and high rate limits, it is thus possible to calculate the effect of nuclear uncertainties on the light element yields. Recently, two other SBBN calculations have been performed: one based on the Nollett and Burles (NB) [10] compilation and another on a partial reanalysis the NACRE data by Cyburt, Fields, and Olive (CFO) [11]. The NB and NACRE compilations differ in several aspects. The NB compilation addresses primordial nucleosynthesis while NACRE is a general purpose compilation. Consequently, NB contains a few more reactions of interest to BBN and a few more data in the energy range of interest. Also, *from the statistical point of view*, the rate uncertainties are better defined in NB, however the astrophysical S factors[2] are fitted by splines which have no physical justification and can produce local artifacts by following to closely experimental data points. On the contrary, the NACRE compilation spans wider energy ranges, and over these ranges, the S factors are fitted to functions based on theoretical assumptions.

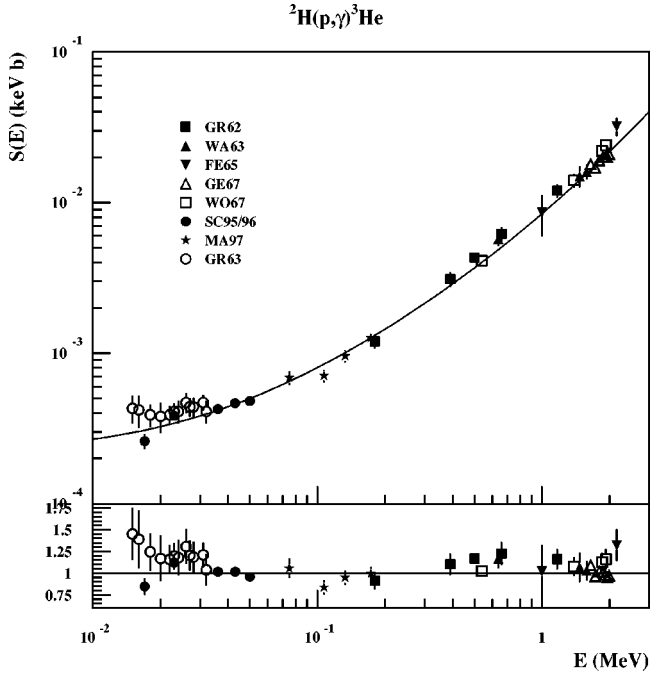

FIG. 2. Upper panel: astrophysical S factor for the ^{2}H$(p,\gamma)^3$He reaction (adapted from NACRE [6], for references see NACRE except for SC96 [51].) Lower panel: relative dispersion of residuals ($S_{\rm exp}/S_{\rm fit}$).

Figure 2 shows that outside of resonances a simple fit (second order polynomial in this case) is sufficient to account for ≈ 2 orders of magnitude variation in S. For the D$(p,\gamma)^3$He reaction, as in Ref. [18], we use the revised data of Schmidt *et al.* [51] (SC96 in Fig. 2) not considered in NACRE. The lower panel displays the ratio between the experimental and fitted S values. The dispersion around unity is small and can hardly be considered physical. It should be noted that by using such a simple fit (when permitted by theory), precise data points outside the range of BBN energy (e.g., the high energy data point in this case) helps constrain the fitted S factor in the region of interest (~ 0.1 MeV in this case). This eliminates spurious local effects induced by a few erratic data points associated with experimental problems rather than a genuine physical effect. For instance, Fig. 3 (adapted from NACRE [6]) shows the nuclear data and the NACRE recommended S factor for the ^{7}Li$(p,\alpha)^4$He reaction can be compared with Fig. 12 of NB [10]. In this latter analysis, the S factor is unduly influenced by the Harmon

[2]The astrophysical S factor is defined by $\sigma(E) \equiv [S(E)/E]\exp(-2\pi\eta) \equiv [S(E)/E]\exp(-\sqrt{E_G/E})$ where here η ($= Z_1 Z_2 e^2/\hbar v$) is the Sommerfeld parameter. It reduces the strong dependency of the cross section (σ) at low energy by approximatively correcting for the penetrability of the Coulomb barrier.

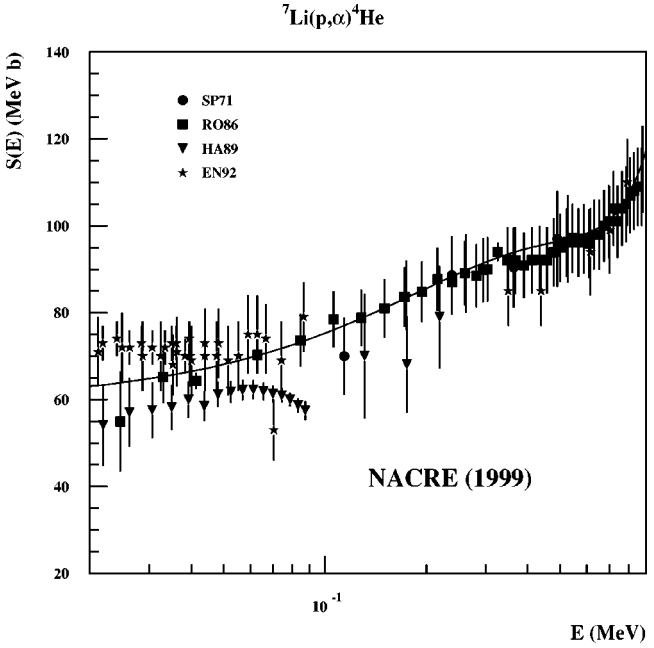

FIG. 3. Astrophysical S factor for the $^7\mathrm{Li}(p,\alpha)^4\mathrm{He}$ reaction (adapted from NACRE [6]). For references other than HA89 [52] and RO86 [53], see NACRE.

[52] data which is a measurement relative to the assumed constant S factor of the $^6\mathrm{Li}(p,\alpha)^3\mathrm{He}$ reaction. The rise of S at low energy is also more likely interpreted by the effect of atomic electron screening of the nucleus. In this energy range, the cross section is expected to be non resonant, mainly determined by the tails of higher energy resonances. This is why, NACRE has constrained S to follow a low order polynomial with the consequence that the good and extensive data provided by Rolfs and Kavanagh [53] are better taken into account. In some cases [e.g., the $\mathrm{D}(d,n)^3\mathrm{He}$ reaction] the NB compilation provides more data points in the region of interest than NACRE. However, considering a wider energy range, NACRE relies on an interpolation between high and low energy data. It is difficult to further compare the reaction rates obtained in both compilations because NACRE provides reaction rate limits (and in some cases S factors) that can be used for e.g., subsequent Monte Carlo calculations, while in NB the rate calculation and Monte Carlo cannot be disentangled. Indeed, in NB, the Monte Carlo procedure is not applied to the rates but to the data points within experimental errors followed by spline fitting. This method is expected to take better into account experimental errors but is difficult to evaluate especially because it could depend on the partitions of the energy interval used for spline fitting which are not given. Nevertheless the final results (i.e., ^{4}He, D, ^{3}He, and ^{7}Li yields) are in good agreement [49] showing that both approaches are valid. CFO [11] have reanalyzed the compiled data from NACRE using the same S factor energy dependences but leaving the scaling factors free. They found that global normalization factors were slightly different from the NACRE ones. As the fitting procedure is straightforward, the origin for this difference is difficult to interpret. One possibility is that a few data points were excluded by NACRE due to suspected experimental problem or physical bias (screening at low energy). CFO [11] subsequently determined scaling factors for each experiment to take into account systematics. From the dispersion of these factors they obtained a better evaluation of rate uncertainties including systematic effects. These analyses underestimate the fact that data on experimental cross sections are in general of much better quality at BBN energy or above than at lower energies. Indeed the cross sections for charged particle reactions drop very rapidly at low energy (Coulomb barrier) making experiments more and more difficult and hence subject to systematic errors. In addition screening of the nucleus by atomic electrons is known to affect cross sections at low energy [54]. Hence, a scaling factor obtained from a low energy measurement is likely to be more affected by systematic errors that another one derived from a high energy data set, even if the quality of the fits is the same. This could affect the calculated CFO systematic error contribution.

Clearly those recent compilations or analyses [7,6,10,11] have all improved the determination of BBN rates and rate uncertainties but more progress could be made. This would include a better theoretical determination of the energy dependence of S factors sometimes just assumed to be a low order polynomial. This would improve the constraint given by the shape of $S(E)$. Such work is under way [55].

Because of the difficulty of defining a universal statistical method for the wide set of reactions (each with its peculiarities) and range of temperature, the NACRE rate limits correspond to upper and lower bounds rather than standard deviations. Accordingly, we assumed a uniform distribution for the rates between the limits (keeping the mean rates equal to the recommended rates).

Four reactions of interest to BBN are not found in the NACRE compilation of *charged* particle induced reactions. They are the neutron induced reactions $n \leftrightarrow p$, $^1\mathrm{H}(n,\gamma)^2\mathrm{H}$, $^3\mathrm{He}(n,p)^3\mathrm{H}$, $^7\mathrm{Be}(n,p,)^7\mathrm{Li}$ and also $^3\mathrm{He}(d,p)^4\mathrm{He}$. The first reaction governs the neutron-proton ratio at the time of freeze-out and hence directly the ^{4}He primordial abundance. The main source of uncertainty on this rate used to be the neutron lifetime but its value is now precisely (886.7 ± 1.9 s) known [56]. So even though improved theoretical calculations [57] may introduce small corrections, this reaction is now sufficiently known for BBN calculations. The following reaction, $^1\mathrm{H}(n,\gamma)^2\mathrm{H}$, also relies almost exclusively on theory. A new calculation including quoted uncertainties has been made available recently [9]. For this reaction, the uncertainties arising from the experimental input data (one low-energy normalization value for the cross section) are expected to be much smaller than those from theory. The errors are given by the order of the first neglected terms in the expansion [9]. To derive the reaction rate and its limits, we performed numerical integrations using the analytical formulas for the cross section and its calculated uncertainties [9]. As there is no way to determine the statistical distribution of these *theorical errors* we adopted (as for NACRE) a uniform distribution as for the following reaction. Following discrepancies and lack of documentation for the $^3\mathrm{H}(p,n)^3\mathrm{He}$ reaction and its inverse, a new and precise measurement has recently been performed [8]. The re-

sults corroborate the cross section provided by the ENDF/B-VI evaluation of neutron data [58] leading to an estimated uncertainty of 5% [8]. For the two remaining reactions ^{3}He$(d,p)^4$He and ^{7}Be$(n,p)^7$Li no new measurements are available and we adopt accordingly the reaction rate and uncertainties provided by Smith, Kawano and Malaney [7]. (In the more recent NB analysis the reaction rates and uncertainties are not available due to the intricate coupling of the fitting and Monte Carlo methods.) They performed an R-matrix analysis (a standard nuclear physics method to tackle resonant reactions) complemented by polynomial fits to the data. Their quoted 1σ uncertainties are respectively 8 and 9% [7] and we use accordingly for these two reactions a Gaussian distribution of errors.

V. RESULTS

In a first step, we complemented our previous analysis [18], limited to NACRE reactions, by calculating the influence of individual reaction rates on ^{4}He, D, ^{3}He and ^{7}Li yields. Then we calculated the maximum of the quantity $\Delta N/N \equiv N_{high}/N_{low} - 1$ within the range of η_{10} variations for each of the 4 isotopes. Positive (resp. negative) values correspond to higher (resp. lower) isotope production when the high rate limit is used instead of the low one (see Ref. [18]). Results are displayed in Table I.

Then we performed Monte Carlo calculations with the rate distributions discussed above. For each η value, we calculated the mean value and standard deviation (σ) of the ^{7}Li yield distribution. The corresponding $\pm 2\sigma$ limits are represented in Fig. 4. In Fig. 5 is represented the likelihood functions for ^{7}Li only $[\mathcal{L}^7(\eta)]$, D only $[\mathcal{L}^2(\eta)]$ and for both $[\mathcal{L}^{7,2}(\eta)]$. The $n\sigma$ confidence intervals (see Table II) are obtained by solving $\ln(\mathcal{L}(\eta)) = \ln(\mathcal{L}_{\max}) - n^2/2$, for η. To calculate $\mathcal{L}$, we use the abundance distributions obtained by Monte Carlo together with a normal distribution associated with the adopted primordial abundances. Following the conclusions of Sec. II, we assumed that the primordial ^{7}Li abundance is such that $\log(^7\text{Li/H})$ is normally distributed with mean -9.91 and standard deviation $\sigma = 0.19/2$ as given by Ryan *et al.* [36]. We neglected the asymmetry in the error bars ($-9.91^{+0.19}_{-0.13}$ [36]) by taking the largest because the smallest concerns the ^{7}Li lower limit that only affects the $\mathcal{L}^7$ central dip, and not the η limits (Fig. 4 lower panel). Unfortunately, the U shape of the ^{7}Li curve together with the Ryan *et al.* [36] values leads to a merging of the low and high η intervals. For comparison, we also show the likelihood function obtained when using the Bonifacio and Molaro [30] older value exhibiting two η intervals. Their merging clearly originates from the new lower primordial abundance obtained when correcting for the apparent ^{7}Li/H versus metallicity slope (see Fig. 1 and Sec. II). From this curve, we obtain for $\Omega_b h^2$, the range 0.006–0.016 (95% C.L., ^{7}Li only).

To calculate $\mathcal{L}^2$, the likelihood function concerning D only, we adopted the highest observed value [20] (see Sec. II). The $\mathcal{L}^2$ curve (Fig. 5) is centered on $\eta = 5 \times 10^{-10}$ and is only marginally consistent with the $\mathcal{L}^7$ one. The situation is even worse if the smaller values of the D primordial abundances are considered. The agreement between SBBN and the ^{7}Li and D observed primordial abundances is impressive when considering the orders of magnitude involved but remains only moderately good when trying to determine the $\Omega_b h^2$ value. The global $\mathcal{L}^{2,7}$ likelihood function provide $\Omega_b h^2 = 0.015 \pm 0.003$ (2σ) which is reasonably compatible with the BOOMERANG [43] ($\Omega_b h^2 = 0.022^{+0.004}_{-0.003}$; 1σ), and DASI [41] ($\Omega_b h^2 = 0.022^{+0.007}_{-0.006}$; 2σ) values. However, as discussed above this is based on unsettled discrepancies on the ranges dictated separately by ^{7}Li and D. Better agreement between SBBN and CMB has been claimed in other works [59]: $\Omega_b h^2 = 0.020 \pm 0.002$ (95% C.L.). This result from the choice of smaller D primordial abundances, drives $\Omega_b h^2$ to higher values but at the expense of compatibility with ^{7}Li. Considering that the chemical evolution of D from BBN to present is not well known, but given that it can only be destroyed in this process, our choice of adopting the higher observed value seems justified. However, a better compatibility with the more reliably determined primordial ^{7}Li abundance would even favor a possible higher D abun-

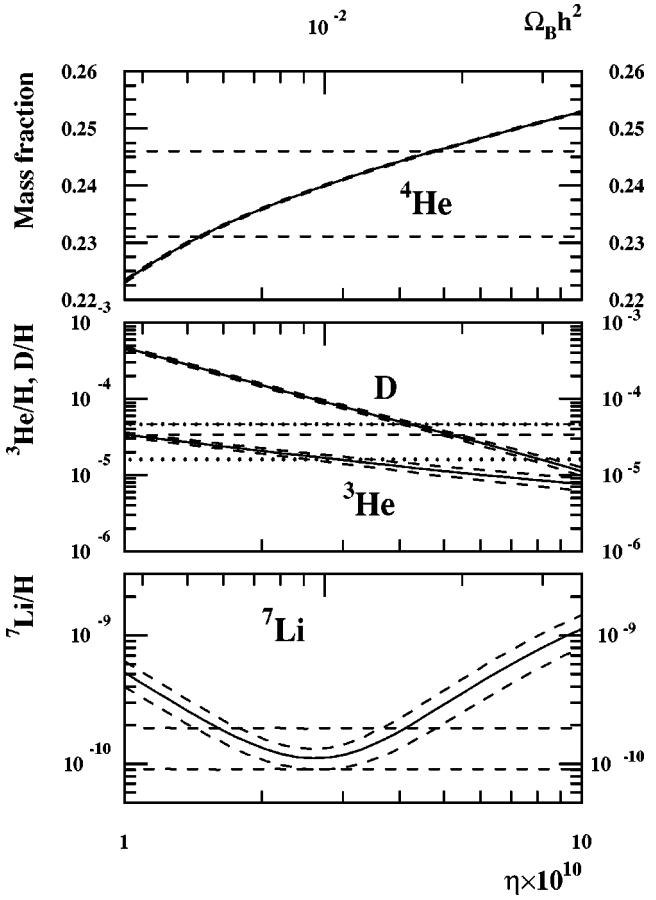

FIG. 4. Abundances of ^{4}He (mass fraction), D, ^{3}He, and ^{7}Li (by number relative to H) as a function of the baryon over photon ratio η. Mean values (solid curves) and 2σ limits (dashed curves) are obtained from Monte Carlo calculations. Horizontal lines represent primordial ^{4}He, D, and ^{7}Li abundances deduced from observations (see text). For D the dotted lines represent the range of observed values (see Fig. 1) while the dashed lines corresponds to the adopted value of Ref. [20].

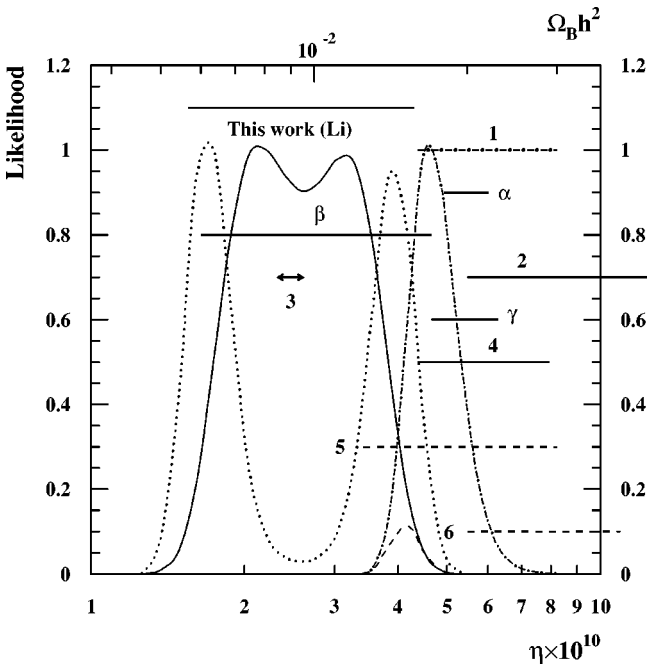

FIG. 5. Likelihood function for ^{7}Li, D, ^{7}Li+D and η ranges from CMB, Lyman-α and other SBBN calculations. The horizontal lines represent $\Omega_b h^2$ and η intervals: 2σ confidence limits (solid lines), twice the 1σ limits (dash-dotted line) or statistically less well defined limits (dashed lines and arrows). Labels (α, β, . . . ,5, 6) point to the last column of Table II where more details are given. The solid curve represents $\mathcal{L}^7$ for the adopted value of ^{7}Li primordial abundance while the dotted curve displays $\mathcal{L}^7$ if the higher value of Bonifacio and Molaro [30] is adopted. The likelihood function for D ($\mathcal{L}^2$, dash dotted curve) is only marginally consistent with $\mathcal{L}^7$ as shown by $\mathcal{L}^{7,2}$ (dashed curve). [$\mathcal{L}^2$ and $\mathcal{L}^7$ have been normalized to $\mathcal{L}_{\max}=1$.]

dance, implying that D has already been partially destroyed in the cosmological cloud. Of course this would decrease the compatibility with CMB observations.

VI. CONCLUSION

Big bang nucleosynthesis has been the subject of permanent interest since it gives access to the baryon density which is a key cosmological parameter. Though independent methods are now available, the SBBN one remains the most reliable because (i) the underlying physics is well known and (ii) there is essentially only one free parameter contrary to other methods. It is worth pursuing the improvement of nuclear reaction rates and abundance determination of light elements, essentially D and ^{7}Li.

Our SBBN results, $\Omega_b h^2 = 0.006$–0.016 based on ^{7}Li only and 0.015 ± 0.003 with D are good agreement with those from Cyburt *et al.* [60]. The $\Omega_b h^2$ value derived by Burles, Nollett and Turner [59] (D and ^{7}Li) is in reasonable agreement with ours. These results are broadly consistent with the CMB ones (MAXIMA, BOOMERANG and DASI) and those obtained via the observation of the Lyman-α forest at high redshift (see also Cyburt *et al.* [60]). However, the SBBN values derived separately from ^{7}Li and D are only marginally compatible and when using the more reliable indicator, lithium, the agreement with the CMB and Lyman-α values is also marginal.

TABLE II. Comparison of $\Omega_b h^2$ from different methods. Limits are given for 2σ except for values in italic (see table footnotes). The last column provides the labels for the $\Omega_b h^2$ ranges displayed in Fig. 5.

Method	$\Omega_b h^2$	Fig. 5
SBBN+Obs (Li), this work	0.006 – 0.016	
SBBN+Obs (Li+D), this work	0.015 ± 0.003	
SBBN from Burles *et al.*[a]	0.020 ± 0.002	α
SBBN from CFO[b] He + Li	0.006 – 0.017	β
SBBN from CFO[b] low D	0.017 – 0.023	γ
CMB BOOMERANG[c]	$0.022^{+0.008}_{-0.006}$	1
CMB from MAXIMA[d]	0.0325 ± 0.0125	2
CMB from CBI[e]	≈ 0.009	3
CMB from DASI[f]	$0.022^{+0.007}_{-0.006}$	4
Lyman-α[g]	0.0125 – 0.03	5
Lyman-α[h]	0.03 ± 0.01	6

[a]Burles, Nollett, and Turner (2001) [59].
[b]Cyburt *et al.* (2001) [11].
[c]de Bernardis *et al.* (2001) [43]; 2σ interval approximated by twice the width of the 1σ interval.
[d]Stompor *et al.* (2001) [47].
[e]Padin *et al.* (2001) [40]; no confidence interval given.
[f]Pryke *et al.* (2001) [41].
[g]Riediger *et al.* (1998) [4]; estimated range of values from Petitjean (2001) [28].
[h]Scott *et al.* (2000) [45] and Hui *et al.* (2001) [44]; no details on statistical significance given.

It is interesting to note that the SBBN [10,18,11] results derived from the two recent and *independent* reaction rate compilations (NACRE [6] and NB [10]) agree very well. Progress in the derivation of primordial abundances (D) are certainly needed, but improvement in the determination of nuclear reaction rates would also be of interest (^{7}Li nucleosynthesis specifically). Concerning this last point, reanalysis of existing data constrained with improved theoretical input is under way [55]. However, it would be even more important that new experiments dedicated to precise and systematic measurements (e.g., in Refs. [53,8]) of the lesser known cross section (Table I) be undertaken.

ACKNOWLEDGMENTS

We are deeply indebted to Roger Cayrel and Patrick Petitjean for illuminating discussions. We warmly thank Brian Fields and Keith Olive for the permanent collaboration on the light elements. We also thank Carmen Angulo and Pierre Descouvemont for clarifying discussion on the NACRE methodology and Dave Lunney for a careful reading of the manuscript. This work has been supported by the PICS number 1076 of INSU/CNRS.

[1] D. N. Schramm and M. S. Turner, Rev. Mod. Phys. **70**, 303 (1998).
[2] W. Hu, N. Sugiyama, and J. Silk, Nature (London) **386**, 37 (1997).
[3] F. R. Bouchet, P. Peter, A. Riazuelo, and M. Sakellariadou, Phys. Rev. D **65**, 021301(R) (2002).
[4] R. Riediger, P. Petitjean, and J. P. Mücket, Astron. Astrophys. **329**, 30 (1998).
[5] J. W. Wadsley, C. J. Hogan, and S. F. Anderson, in *Clustering at High Redshift*, ASP Conference Series Vol. 200, 2000, edited by A. Mazure, O. Le Fèvre, and V. Le Brun, p. 291.
[6] C. Angulo *et al.*, Nucl. Phys. **A656**, 3 (1999).
[7] M. S. Smith, L. H. Kawano, and R. A. Malaney, Astrophys. J., Suppl. Ser. **85**, 219 (1993).
[8] C. R. Brune, K. I. Hahn, R. W. Kavanagh, and P. W. Wrean, Phys. Rev. C **60**, 015801 (1999).
[9] J.-W. Chen and M. J. Savage, Phys. Rev. C **60**, 065205 (1999).
[10] K. M. Nollett and S. Burles, Phys. Rev. D **61**, 123505 (2000).
[11] R. H. Cyburt, B. D. Fields, and K. A. Olive, New Astron. **6**, 215 (2001).
[12] K. A. Olive and E. Skillman, New Astron. **6**, 119 (2001).
[13] B. D. Fields and K. A. Olive, Astrophys. J. **506**, 177 (1998).
[14] Y. I. Izotov and T. X. Thuan, Astrophys. J. **500**, 188 (1998).
[15] M. Peimbert, A. Peimbert, and M. T. Ruiz, Astrophys. J. **541**, 688 (2000).
[16] D. Kirkman *et al.*, Astrophy. J. **559**, 23 (2001).
[17] J. K. Webb, R. F. Carswell, K. M. Lanzettas, R. Ferlet, M. Lemoine, A. Vidal-Madjar, and D. V. Bowen, Nature (London) **383**, 250 (1997).
[18] E. Vangioni-Flam, A. Coc, and M. Cassé, Astron. Astrophys. **360**, 15 (2000).
[19] B. D. Fields, K. A. Olive, J. Silk, M. Cassé, and E. Vangioni-Flam, Astrophys. J. **563**, 653 (2001).
[20] S. Burles and D. Tytler, Astrophys. J. **507**, 732 (1998).
[21] J. M. O'Meara, D. Tytler, D. Kirkman, N. Suzuki, J. X. Prochaska, D. Lubin, and A. M. Wolfe, Astrophys. J. **552**, 718 (2001).
[22] S. D'Odorico, M. Dessauges-Zavadsky, and P. Molaro, Astron. Astrophys. **368**, L21 (2001).
[23] M. Pettini and D. V. Bowen, Astrophys. J. **560**, 41 (2001).
[24] S. A. Levshakov, M. Dessauges-Zavadsky, S. D'Odorico, and P. Molaro, Astrophys. J. (to be published), astro-ph/0105529.
[25] A. Vidal-Madjar, in *Cosmic Evolution*, edited by E. Vangioni-Flam, R. Ferlet, and M. Lemoine (World Scientific, Singapore, 2001), p. 49.
[26] J. Geiss and G. Gloeckler, Space Sci. Rev. **84**, 239 (1998).
[27] J. L. Linsky, Space Sci. Rev. **84**, 285 (1998).
[28] P. Petitjean (private communication).
[29] F. Spite and M. Spite, Astron. Astrophys. **115**, 357 (1982).
[30] P. Bonifacio and P. Molaro, Mon. Not. R. Astron. Soc. **285**, 847 (1997).
[31] S. G. Ryan, J. Norris, and T. C. Beers, Astrophys. J. **523**, 654 (1999).
[32] S. G. Ryan, T. Kajino, T. C. Beers, T. K. Suzuki, D. Romano, F. Matteucci, and K. Rosolankova, Astrophys. J. **549**, 55 (2000).
[33] E. Vangioni-Flam, M. Cassé, R. Cayrel, J. Audouze, M. Spite, and F. Spite, New Astron. **4**, 245 (1999).
[34] S. Theado and S. Vauclair, Astron. Astrophys. **375**, 70 (2001).
[35] R. Cayrel, M. Spite, F. Spite, E. Vangioni-Flam, M. Cassé, and J. Audouze, Astron. Astrophys. **343**, 923 (1999).
[36] S. G. Ryan, T. C. Beers, K. A. Olive, B. D. Fields, and J. E. Norris, Astrophys. J. Lett. **530**, L57 (2000).
[37] A. Balbi *et al.*, Astrophys. J. Lett. **545**, L1 (2000); **558**, L145 (2001).
[38] A. E. Lange *et al.*, Phys. Rev. D **63**, 042001 (2001).
[39] A. H. Jaffe *et al.*, Phys. Rev. Lett. **86**, 3475 (2001).
[40] S. Padin *et al.*, Astrophys. J. Lett. **549**, L1 (2001).
[41] C. Pryke, N. W. Halverson, E. M. Leitch, J. Kovac, J. E. Carlstrom, W. L. Holzapfel, and M. Dragovan, astro-ph/0104490.
[42] P. A. R. Netterfield *et al.*, astro-ph/0104460.
[43] P. de Bernardis *et al.*, astro-ph/0105296.
[44] F. Hui, Z. Haiman, M. Zaldarriaga, and T. Alexander, astro-ph/0104442.
[45] J. Scott, J. Bechtold, and A. Dobrzycki, Astrophys. J., Suppl. Ser. **130**, 67 (2000).
[46] C. C. Steidel, M. Pettini, and K. L. Adelberger, Astrophys. J. **546**, 665 (2001).
[47] R. Stompor *et al.*, Astrophy. J. Lett. **561**, L7 (2001).
[48] E. Vangioni-Flam, A. Coc, and M. Cassé, Nuclei in the Cosmos 2000, Proceedings [Nucl. Phys. **A688**, 393 (2001)].
[49] A. Coc, E. Vangioni-Flam, and M. Cassé, in *Cosmic Evolution*, [25], p. 35.
[50] G. R. Caughlan and W. A. Fowler, At. Data Nucl. Data Tables **40**, 283 (1988).
[51] G. J. Schmidt *et al.*, Nucl. Phys. **A607**, 139 (1996).
[52] J. F. Harmon, Nucl. Instrum. Methods Phys. Res. B **40/41**, 507 (1989).
[53] C. Rolfs and R. W. Kavanagh, Nucl. Phys. **A455**, 179 (1986).
[54] C. Angulo, S. Engstler, G. Raimann, C. Rolfs, W. H. Schulte, and E. Somorjai, Z. Phys. A **345**, 231 (1993).
[55] P. Descouvemont *et al.* (in preparation).
[56] Particle Data Group, D. E. Groom *et al.*, Eur. Phys. J. C **15**, 1 (2000).
[57] L. S. Brown and R. F. Sawyer, Phys. Rev. D **63**, 083503 (2001).
[58] ENDF/B-V, National Nuclear Data Center, Brookhaven National Laboratory, Upton, New York (http://www.nndc.bnl.gov/nndc/endf/).
[59] S. Burles, K. M. Nollett, and M. S. Turner, Astrophys. J. Lett. **552**, L1 (2001).
[60] R. H. Cyburt, B. D. Fields, and K. A. Olive, New Astron. **6**, 215 (2001).